ФІЗИКА І ХІМІЯ ТВЕРДОГО ТІЛА
Т. 5, № 4 (2004) С. 849-858

PHYSICS AND CHEMISTRY OF SOLID STATE
V. 5, № 4 (2004) P. 849-858

PACS 42.88. +h

ISSN 1729-4428

Tomasz Boczar

Results of Time-Frequency Analysis of Acoustic Emission Pulses Generated by Surface Partial Discharges in Air

Technical University of Opole, Poland

The subject matter of this paper covers the issues connected with the application of modern numerical methods in processing and analysis of the signals measured by the acoustic emission (AE) method during high-power experiments carried out in laboratory conditions in set-up modeling surface partial discharges (PDs) in air.

First of all, the paper presents the results of the time-frequency analysis of the AE pulses generated by PDs carried out using continuous (CWT) and discrete (DWT) wavelet transforms as well as a STFT transformation. Moreover, it presents the runs of the power density spectra and columnar diagrams showing the size of the energy transferred at the particular decomposition levels.

Keywords: time-frequency analysis, discharges, acoustic emission.

Стаття поступила до редакції 19.05.2004; прийнята до друку 31.08.2004.

I. Introduction

At present the acoustic emission (AE) method is a significant supplement of the measurement methods used in diagnostics of insulation systems of power appliances. It makes it possible to take measurements in industrial conditions without the need to disconnect operating devices from the power system. The information obtained through using the AE method refers to the amount, intensity and, to some extent, to the location of partial discharge (PD) occurrence in the insulation systems under study.

In practical usage there exists a large number of insulation systems built in such a way that solid dielectrics constantly cooperate with liquid and gas dielectrics. The plane separating the cooperating dielectrics is usually the place in which the electric strength of the whole system is the lowest. Along this surface there can occur surface electric partial discharges or disruptive discharges which lead to the insulation breakdown. The occurrence and development of surface partial discharges (SPDs) depends mainly on the kind and the surface condition of a solid dielectric, the kind of the system supplying voltage and the special intensity distribution of an electric field. Also, the resistance of a solid dielectric to the occurrence of PDs on its surface is very significant. These properties are conditioned by the internal structure of a solid dielectric, and most of all by the existence of a dirt layer on its surface. Such dielectrics as glass and porcelain do not participate actively in the occurrence and development of SPDs, contrary to dielectrics of an organic origin.

The classic example of a diagonally layered system is a bushing insulator. The voltage distribution in such insulation system depends first of all on the surface capacity and the capacity of a dielectric placed between electrodes. The stand-off insulator is the simplest example of an insulation system layered parallel, in which the electric field intensity on both sides of the boundary surfaces in each dielectric is of the same value. At the same electric field intensities the electric spark-over takes place in a dielectric of a lower strength. The equivalent circuit diagrams of such systems, equations describing the physics of the phenomena analyzed, and the diagrams presenting the dependencies of the voltage jump on the spacing between the electrodes have been widely discussed, among others, in the works [22,42].

The aim of the research carried out--the results of which are presented in this paper-- was to perform a time-frequency analysis using a STFT and continuous and discrete wavelet transforms of the AE pulses generated in a cylinder-plane spark gap with a layer of glass insulation placed between the electrodes, which made the modelling of surface partial discharges possible.

II. Characteristics of the set-up for generation and measurement of the ae from surface discharges

The set-up generating surface discharges (Fig. 1) consisted of a metal electrode in the shape of a cylinder, to which high voltage was attached, the insulation layer was six glass planes 0.54 mm thick each, and an aluminium plane, which was grounded. The set-up was

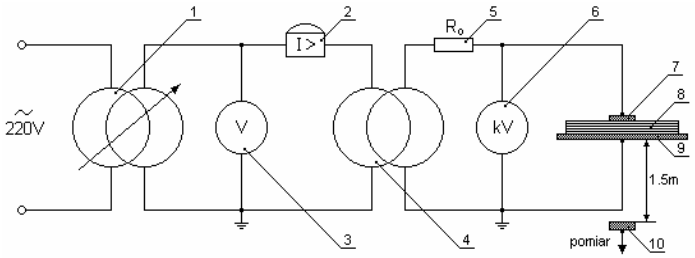

Fig. 1. Diagram of the set-up for surface discharge generation: 1 – autotransformer, 2 – over-current relay, 3 – digital voltometer, 4 – test transformer, 5 – resistor, 6 – electrostatic voltometer, 7 – high voltage electrode, 8 – insulation planes made of glass, 9 – grounded electrode, 10 – measuring transducer.

supplied by an alternating voltage of a root-mean-square value equal to 32 kV, which was 80% of the breakdown voltage value of the spark gap. The high voltage was obtained from a test transformer of a transformer voltage ratio equal to 220/110000 V/V. The set-up under study generated SPDs, the AE of which was measured by a measuring transducer placed 1.5 m away from the spark gap. Te AE pulses generated by SPDs were registered using a standard measuring set-up by the Brüel&Kjæl firm consisting of a wideband contact piezoelectric transducer, an amplifier, a filter and a measuring card, the detailed characteristics of which have been presented in the work [13,14].

The diagram of the set-up used for generation of corona discharges was presented in Fig. 1.

III. Time-frequency analysis

The AE pulses generated by PDs are characterized by a wide frequency spectrum dependent on a discharge type. Moreover, they are characterized by a big change dynamics in the time domain. The methods of the acoustic signal analysis used so far were based on the analyses either in time or frequency domains [8,9]. This approach does not fully reflect the character of the AE pulses generated, thus the author of the paper have suggested a Joint Time-Frequency Analysis (JTFA). The time-frequency analysis is a useful and required tool for examining non-stationary signals the parameters of which change in time, and that is why it is now used in the electric method of insulation measurement and it can be used for evaluation of the AE pulses generated by PDs [48-50]. The presentation of the AE pulses measured on a time-frequency ground enables not only a spectrum analysis resulting from time changes but it can also be a helpful tool used for determining the kind and size of the accompanying disturbances. Moreover, the use of the time-frequency analysis limits, to a great extent, the effect of a spectrum broadening connected with the application of the Fast Fourier Transform (FFT) without analyzing windows, which is caused by the phenomenon of overlapping of their fragments.

In the case of non-stationary signals the frequency analysis based on the Fast Fourier Transform makes it possible to determine spectrum characteristics in a definite time range. Frequency resolution then depends on the width of the time range analyzed. Limiting the number of data of the time series is connected with the accuracy decrease of the frequency spectra being determined. The spectrum analysis provides information on average amplitude values or powers or energy size of frequency components which are present in a signal processed. The information on time changes of frequency structures, however, can be obtained by applying the spectrum analysis not to the whole time range but to a selected observation window, which is shifted in time. The change of its tracking enables narrowing or widening of time resolution of a spectrum being determined, which takes place at a simultaneous reverse impact on frequency resolution.

There is a trade of the selection of the time and frequency resolution. If h(t) is chosen to have good time resolution, then its frequency resolution must be deteriorated.

The time-frequency localization is limited by the Heisenberg uncertainty principle [46-7]. In 1946 Denis Gabor introduced into a spectrum analysis a sliding smoothing window [8,16], through the introduction of the Gauss tracking function under the integral sign in the Fourier transformation. In signal analysis also other types of observation windows are applied, e.g. Barlet, Hamming, Hanning, Parzen, Blackman windows etc., which due to a different way of smoothing a function limit the effect of a spectrum leak in different ways.

The main role of the window is to damp out the effects of the Gibbs phenomenon that results from truncation of an infinite series.

The short time Fourier transform can be expressed by the following equation:

$$\mathrm{STFT}_x(\tau,\omega) = \int_{-\infty}^{+\infty} h(t-\tau)x(t)e^{-j\omega t}dt\,, \qquad (1)$$

where: τ is a time tracking within a window, ω is pulsation of the component analyzed, and h is the function of a window.

In many typical applications a spectrogram that is a square of the STFT module, which presents the changes of the spectrum density of the signal power in time, is determined for the signals changeable in time. Also, amplitude spectrograms, which are calculated as the STFT module, are often used [16,36].

A significant feature of the STFT transform is identical resolution on the whole frequency axis and the use during the analysis of only one observation window. This is a clear 'wastefulness' in the sense that it is possible to use the information contained in a signal registered since there is no need to use the window of the

same length as the first harmonic. It is this issue that was the basis for the wavelet transformation theory [10,16, 19,25,38,39,44,46].

In recent years, the wavelet transform, which is an alternative method of the time-frequency analysis of signals, has been developing dynamically and has found numerous promising applications in various branches of knowledge, e.g. such as: approximation theory and differential equations, metrology, theory of signals, aerodynamics, acoustics, data compression, geology, seismology, air and marine radiolocation, impulse echonography, material flow detection, research making use of the sonar technology, telecommunication, medicine, mechanics, theory of vibrations and vibroacoustics as well as astronomy and space flights.

The merits of the wavelet transform and the advantages of its application, compared with the Fourier transform can also be applied in the analysis of the phenomena connected with a widely-understood electrotechnology, especially power engineering, where it is used for the analysis of the transient states of electric circuits. It is also used in protective automation, in the analysis of the harmonic in dynamic states of a system, in signal processing used for the evaluation of the electric energy quality indexes, and in identification of disturbances in power systems [1-3,24,26,30,35,38]. Moreover, the wavelet transform is more and more commonly used in diagnostics of insulation systems of high-power appliances made by using the electrical method of PD measurement. It is used, first of all, for the analysis of electrical branching for denoising of voltage signals, and for classification and identification of PD forms [20, 23, 31, 32, 36, 48].

Generally, the common denominator of technical implementations of wavelet transformations is the possibility of non-stationary signal processing and of performing their evaluation based on new descriptors. Hence the potential application area of the time-frequency analysis using the wavelet transforms is very vast and can apply to all measurement a situation in which there is a need to elicit information contained in a frequency spectrum of the signal under study that is changing in time or space. This information can be both an overall shape of a signal's instantaneous spectrum and a coherent amplitude, phase and instantaneous frequency distributions of its components [7, 10, 38, 47, 48].

Within the analyses carried out, the results of which are presented in this paper, apart from the short-time Fourier transform, a wavelet transformation also was done for two basic reasons. Firstly, the use of the wavelet analysis makes it possible to increase the time-frequency resolution. During the signal processing two narrow observation windows can be used at high frequencies, and wide analyzing windows for the low frequencies. The STFT, however, uses various types of observation windows, but of a constant for a given type time length, and in consequence time-frequency resolution, which is constant in the whole time-frequency plane. Since the pulses of the AE generated by PDs can contain both low- and high-frequency components, the wavelet analysis seems to be very useful for evaluating the character of the time-frequency distributions being determined. Secondly, determining the frequency structure using the STFT is accomplished by decomposition of a signal into a certain number of sinusoidal components. In the wavelet analysis, a signal distribution into a series of well-located base functions, called wavelets, is used. Therefore, the results of the wavelet analysis can contribute to broadening and supplementing the knowledge on the time-frequency structures calculated.

To analyze the AE pulses measured, generated by PDs of the surface type, continuous and discrete wavelet transforms were used.

The continuous transform of the signal x(t) can be described by the equation:

$$\mathrm{CWT}_x(b,a) = (x, ш_{ab}) = \int_{-\infty}^{\infty} x(t) \cdot ш_{ab}(t)^* dt, \qquad (2)$$

where: $\mathrm{CWT}_x(b,a)$ – a continuous wavelet transform, x(t) – a signal under study, a – a scale coefficient, connected with stretching or compression a signal in time, and therefore used indirectly for changing the scale of frequency resolution, b – a shift connected with time location, $ш_{ab}(t)$ – a wavelet function representing a wavelet family, * – denotes coupling of a complex function.

The wavelet transform of the signal x(t), like the short-time Fourier transform, is determined by an integral transformation with a base function limited by the processing window. The function $ш_{ab}(t)$ has the same role as the expression $h(t-\phi) \cdot e^{-j2 \cdot p \cdot f \cdot t}$ in the STTFT and defines a wavelet family of:

$$ш_{ab}(t) = \frac{1}{\sqrt{a}} \cdot ш\left(\frac{t-b}{a}\right), \qquad a \in R, \quad b \in R, \quad (3)$$

where: $\frac{1}{\sqrt{a}}$ – a scaling coefficient ensuring maintaining proper power relations, $ш(t)$ – a basic wavelet, also called a mother wavelet [10,21,23,25,33,34,37,41,44].

Basic functions $ш_{ab}(t)$ are most often of an oscillating character, of a limited duration time, of a zero average value, are suppressed on the range limits, and through the analogy to the shape of their run the 'wavelet' term was introduced [18,37-8,40,46]. The family of wavelet functions is characteristic of a similar shape, but its particular representations differ in scale and shift, i.e. in parameters a and b. The continuous wavelet transform presents the correlation of the signal analyzed x(t) with the corresponding wavelet, the result of which is the function defining the degree of their similarity. Due to the shape of their run, wavelet pictures well local changes of the signals analyzed, which is difficult in the case of the Fourier transform, where the family of the functions sine-cosine is used.

In practical time-frequency analyses of acoustic signals, stressing the research on sound, speech and vibroacoustics, a symmetrical wavelet of a sinusoidal run with the Gauss envelope is used most often, which was constructed by Morlet [5-6,37]. It is recommended in calculations using CWT, and therefore it was used for the

needs of the analyses of the AE pulses generated by PDs of the surface type carried out.

The analytic equation of the Morlet wavelet has the form of the dependency:

$$\varphi(t) = e^{-\frac{t^2}{2}} \cdot \cos(5 \cdot t), \tag{4}$$

and the median pulsation is:

$$ш_0 = 2 \cdot \pi \cdot f_0 = 5\,. \tag{5}$$

The shape of its time run is shown in Fig. 2. For the Morlet wavelet the dependency frequency-scale presented in a lineal scale is a hyperbolic function. Using the logarithmic scale the amplitude spectrum run, which is shown in Fig. 3, is of a linear form for various scale values.

With the continuous wavelet transform the scalogram $SCAL_x(b,a)$ (7.16) is connected, the value of which is calculated as a square of the module $CWT_x(b, a)$, in an analogous way as that of the spectrogram for the STFT transformation.

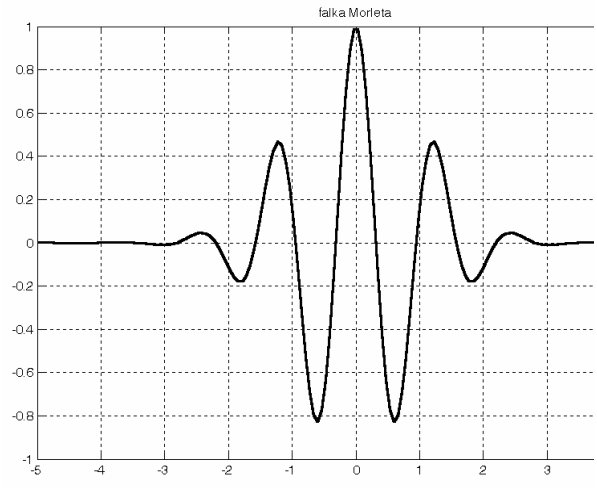

Fig. 2. Morlet wavelet run.

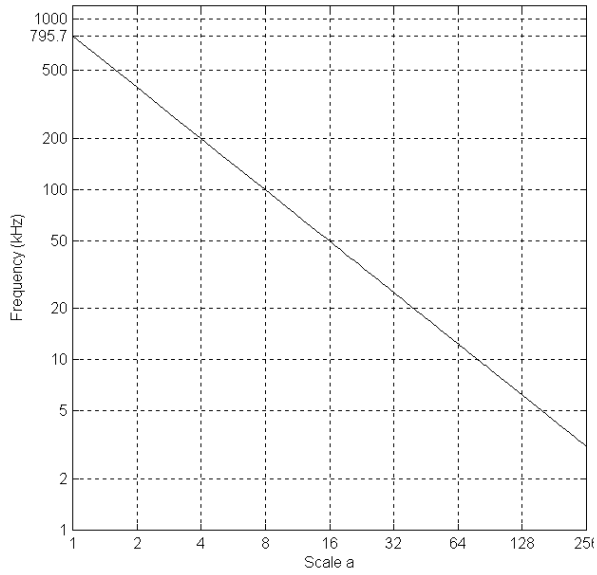

Fig. 3 Frequency dependence on scale for the Morlet wavelet at the sampling frequency of 1 MHz.

$$SCAL_x(b,a) = \left|CWT_x(b,a)\right|^2 \tag{5}$$

where: $SCAL_x(b,a)$ – a scalogram, $CWT_x(b, a)$ – a continuous wavelet transform [47-8].

The scalograms determined by using a continuous wavelet transform contain excess information on the time-frequency structure of the AE pulses measured. In diagnostic systems of insulation systems of power appliances the use of parameters more adapted to expert algorithms is required, which can be applicable in the process of identification and initial PD classification. In this case a more synthetic description is obtained when a discrete form of the wavelet transformation is used.

In the case of the continuous wavelet transform, the scale coefficient a and the shift coefficient b can assume any values, which means that they are continuous functions. However, in the case when the wavelet scale a and the shift b can assume only definite discrete values connected with powers of the number 2 and an exponent that is an integer, i.e. when they are discrete functions, using equation (2) a discrete wavelet transform can be determined. The transformation then is of a dyadic character, which means that the consecutive coefficients are subjects to a double increase, respectively: $a = 2^m$, $b = 2^m \cdot Дt$. In the discrete form scale a is usually substituted by a dyadic scale 2^m, $m \in R$, and then the wavelet family can be presented using the dependency:

$$ш_{mn}(t) = 2^{-m/2} \cdot ш(2^{-m} \cdot t - n) \tag{6}$$

where: value m defines the level of the scale, so also the range of the frequencies analyzed. Value n defines the shift in time equal to $2^m \cdot n$. The increase of the scale m causes an exponential increase of the quantization step of the signal analyzed.

A discrete wavelet analysis of the signal f(t) consists in determining a series $n \in Z$ of the coefficients denoting approximation $a_j[n]$ and details $d_j[n]$. Then the function x(t) is expressed by the equation:

$$x(t) = \sum_{j=-\infty}^{J} \sum_{n \in Z} d_j[n] + \sum_{n \in Z} a_j[n] \cdot \varphi_{jn}, \tag{7}$$

where: $j \in Z$ – a consecutive j decomposition level, J – a number of decomposition levels, φ_{jn} – a scaling function [4, 5, 27, 34].

Within the analyses carried out, the results of which are presented in this paper, apart from the short-time Fourier transform also a wavelet transformation was performed due to two basic reasons. Firstly, the use of the wavelet analysis makes it possible to increase the time-frequency resolution. During the signal processing, narrow observation windows can be sued at high frequencies, and wide analyzing windows for low frequencies. The STFT, however, uses various types of observation windows, but of a constant time length for a given type and, in consequence, of a constant time-frequency resolution. Since the AE pulses generated by PDs can contain both low- and high-frequency components, the wavelet analysis seems to be very useful for evaluating the character of the time-frequency distributions determined. Secondly, determining the frequency structure using the STFT is done through a

signal decomposition into a certain number of sinusoidal components. In the wavelet analysis, however, a signal distribution into a series of well-located base functions, called wavelets, is used. Therefore, the wavelet analysis results can contribute to broadening and supplementing knowledge on the time-frequency structures calculated. Continuous and a discrete wavelet transforms were used for analyzing the AE pulses measured, generated by PDs of the surface type.

Orthonormal symlet base functions were used for multiresolution analysis. Symlet wavelets of a high order ensure the closest approximation at a given level of a precise symmetry and a linear phase. In the case of the analysis carried out, the minimization of the phase distortion was significant in order to keep true time relationships between the details of acoustic pulses, which is why the symlet wavelet 8 was chosen [2,4,8,9, 11-2]. The run of the sym8 wavelet is shown in Fig. 4. For the symlet wavelet the center frequency $ш_0 = p$, and the frequency band $B_0 = p$. For the scales of close values these bands overlap to a great extent. The center frequency and the frequency band corresponding to the particular scales are shown in Fig. 5.

The result of the multiresolution analysis application using a discrete wavelet transform, a set of time approximation runs, and details at various levels were obtained. The particular levels correspond to frequency ranges resulting from the bandwidth of the band-pass filter connected with an analyzing function. The runs obtained constitute a signal decomposition of the pulses measured. Frequency ranges corresponding to the filter bands at various levels are listed in Table 1.

IV. Selected results of measurements and time-frequency analysis of the ae generated by surface discharges

The registered AE pulses of the AE generated by PDs of the surface type underwent a short-time Fourier transform using the Hamming time window. Currently, the Hamming window is commonly used for processing quick-changing signals and is an assumptive function in computer programs which enable the performance of the time-frequency analysis [28-9,45].

For the measured AE pulses generated by PDs of the surface type their corresponding spectrograms were drawn. For presentation of the power density, spectra images in a three-dimensional space were used, and the amplitude spectra were presented as coherent structures in the time-frequency plane and in the time time-frequency-amplitude space. The spectrograms shown in the time-frequency domain were described using a scale in the form of a strip from a pallet of colors, whose particular shades of gray correspond with equivalent amplitude values of the spectrum determined.

Figs 6-11 show spectrograms determined for the AE pulses generated by PDs in air. The spectrograms calculated for the AE pulses generated by PDs at the positive voltage polarization (Fig. 6) are characteristic of

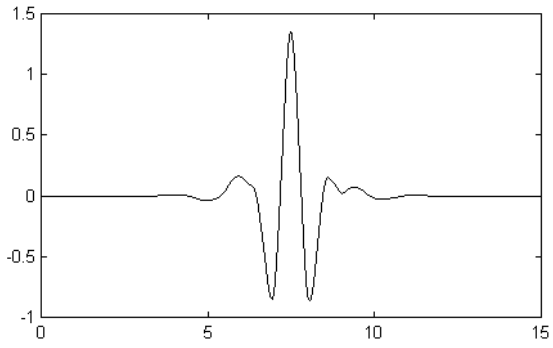

Fig. 4. Symlet wavelet 8 run.

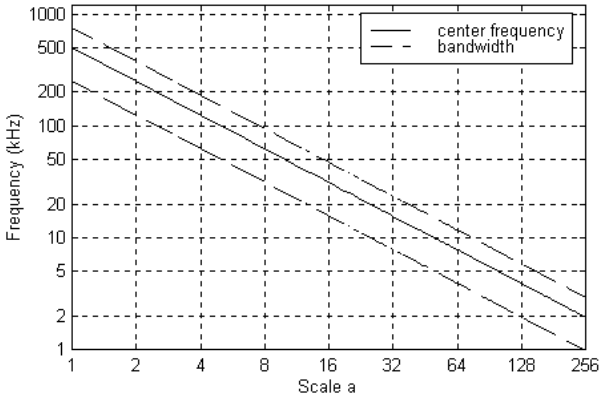

Fig. 5. Dependency of the median frequency and the frequency band on the scale value for the symlet wavelet 8.

Table

Center frequency and bandwidth for the details analyzed

Detail	Center frequency (kHz)	Bandwidth (kHz)
D1	500.0	250-750
D2	250.0	125-375
D3	125.0	62.5-187.5
D4	62.5	31.2-93.7
D5	31.25	15.6-46.8
D6	15.6	7.8-23.4

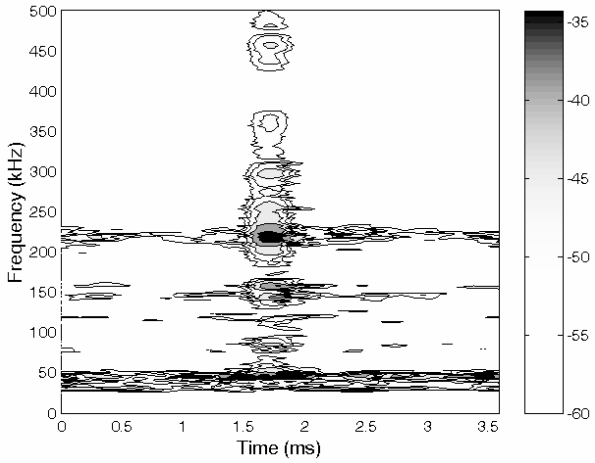

Fig. 6. Spectrogram calculated for the AE pulses generated by PDs in the surface system in air, during the positive voltage half-period.

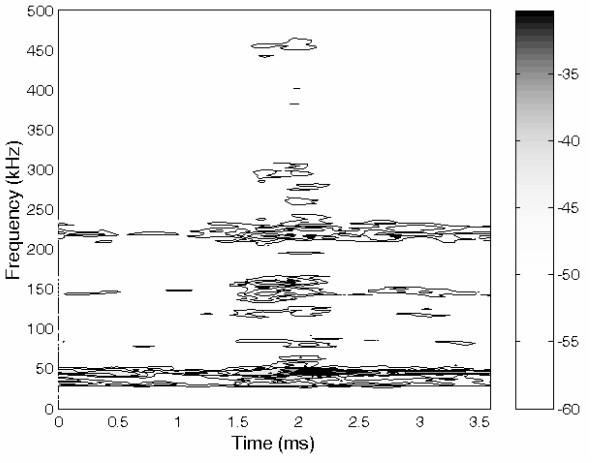

Fig. 9. Spectrogram calculated for the AE pulses generated by PDs in the surface system in air, during the negative voltage half-period.

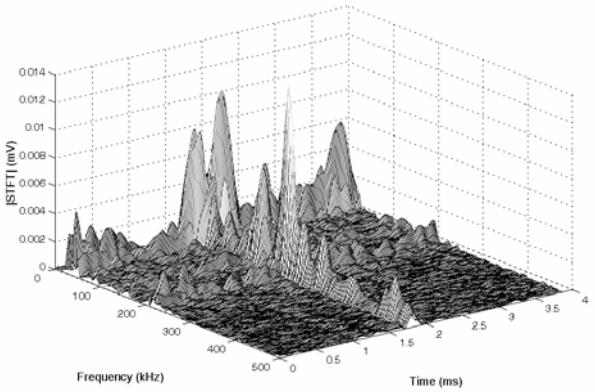

Fig. 7. Three-dimensional spectrogram of amplitude spectrum calculated for the AE pulses generated by PDs in the surface system in air, during the positive voltage half-period.

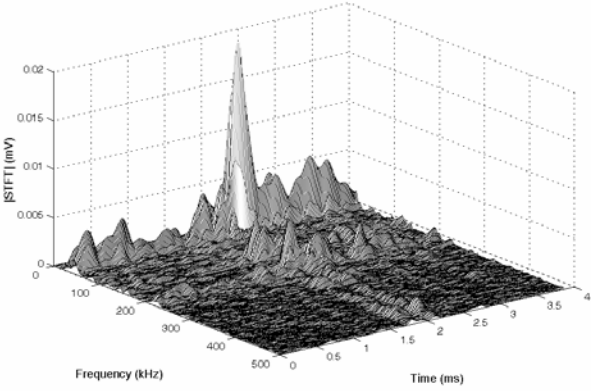

Fig. 10. Three-dimensional spectrogram of amplitude spectrum calculated for the AE pulses generated by PDs in the surface system in air, during the negative voltage half-period.

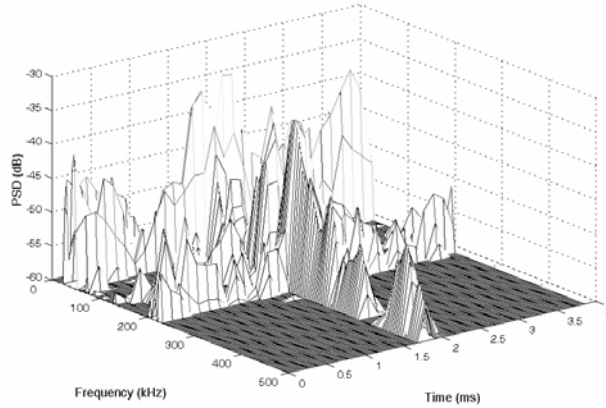

Fig. 8. Three-dimensional spectrogram of power spectrum density calculated for the AE pulses generated by PDs in the surface in air, during the positive voltage half-period.

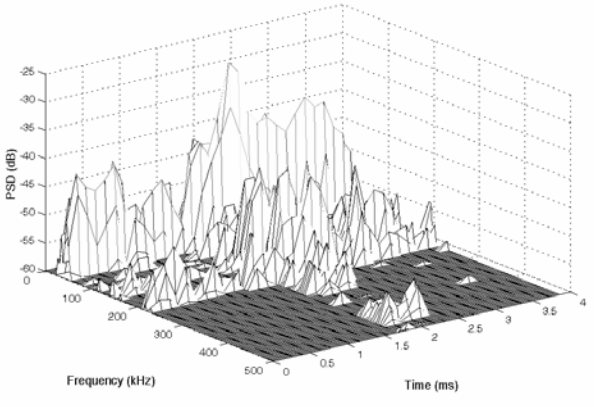

Fig. 11. Three-dimensional spectrogram of power spectrum density calculated for the AE pulses generated by PDs in the surface in air, during the negative voltage half-period.

the occurrence of coherent areas of the frequencies in the range from 70 to 350 kHz and from 450 to 500 kHz. Their duration time is about 0.5 ms and corresponds with the generation time of the AE pulse series from PDs in the time range from 1.5 to 2 ms. Moreover, there occur time-frequency structures in the bands 925-50) kHz and (200-240) kHz. These areas are active in the whole time range analyzed. For the AE pulses generated by PDs in the negative voltage half-time, the distribution of the frequency structures obtained was similar to those obtained in the positive half-time. The run of the spectrogram calculated is shown in Fig. 9.

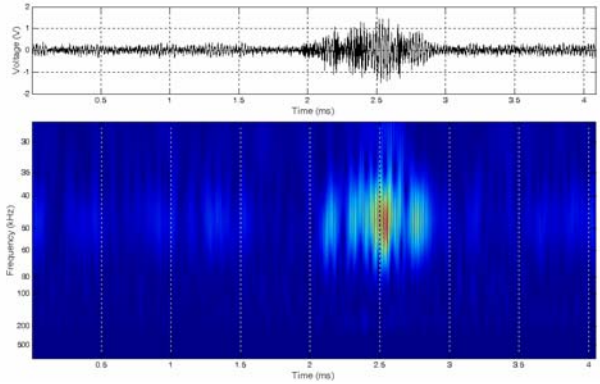

Fig. 12. CWT of a series of AE pulses generated by PDs in oil in the surface system during the positive voltage half-cycle.

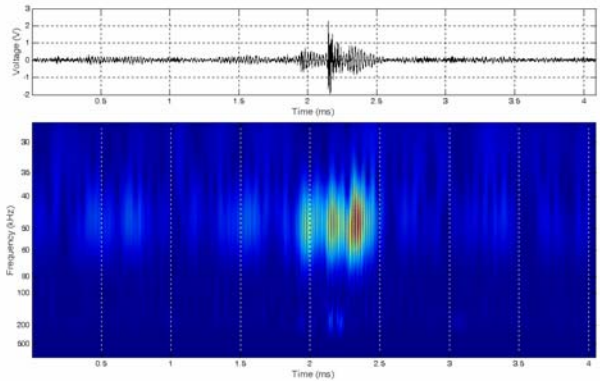

Fig. 13. CWT of a series of AE pulses generated by PDs in oil in the surface system during the negative voltage half-cycle.

Three-dimensional spectrograms shown in Figs 7-8 for the positive voltage polarization and in Figs 10-11 for the negative one confirm the changes of the frequency range of the AE pulses generated. Presenting the spectrogram run in a three-dimensional form makes it possible to determine amplitudes of the particular components. The spectrograms obtained indicate a significantly bigger participation of low-frequency components, which are of a narrow-band noise character in the band from 25 to 50 kHz. This noise is only in an insignificant degree connected with the AE pulses generated by discharges and is rather of a stationary disturbance character. Narrow-band noises also occur in the higher frequency band in the range from 200 to 240 kHz. The amplitudes of the frequency components, however, strictly connected with the occurrence of the AE pulses generated by PDs occur in the time range from 1.5 to 2 ms, and their highest values occur in the band from 20 to 200 kHz. Three-dimensional spectrograms determined for PDs are of a similar character to the frequency structures drawn for both voltage polarizations.

Figs 12-13 show time runs and scalograms determined by using the continuous wavelet transform, of the AE pulses generated by PDs, which are presented separately for the positive and negative voltage polarizations.

The duration time of the time-frequency structures obtained was longer for the AE pulses generated in the positive voltage half cycle, and it was of ca. 1 ms, than for the negative voltage half cycle, which was ca. 0.6 ms. For both voltage polarizations the frequency range in which wavelet structures occur is from 30 to 80 kHz. The images obtained are of a continuous character, in which single wavelet structures cannot be indicated. On the scalograms of the AE pulses determined in both voltage half cycles there also occur structures coherent in the time preceding the PD generation. They are of a narrower frequency range from 40 to 60 kHz, shorter duration time not exceeding 0.4 ms and smaller amplitudes than the time-frequency structures corresponding with the series of the AE pulses for PDs. Moreover, on the scalogram determined for PDs generated in the negative voltage half cycle (Fig. 13) an additional structure is visible in the range from 180 to 220 kHz, but of a smaller amplitude than for the lower frequencies.

The results of the multiresolution analysis obtained for the AE pulses generated by PDs are shown for the positive voltage polarizations in Fig. 14 and for the negative voltage polarizations in Fig. 15. These figures present in order: original time runs of the AE pulses generated by PDs, approximation A on the seventh decomposition level, and details D on the levels from 1 to 7, then power density spectra runs and columnar diagrams visualizing the size of the energy transferred by the particular details. For both voltage polarizations the highest activity is shown by the runs of the highest frequency details from D1 to D3. For the positive polarization these are single structures of the duration time not exceeding 0,2 ms. For the AE pulses generated by PDs in the negative half-time, there occur more

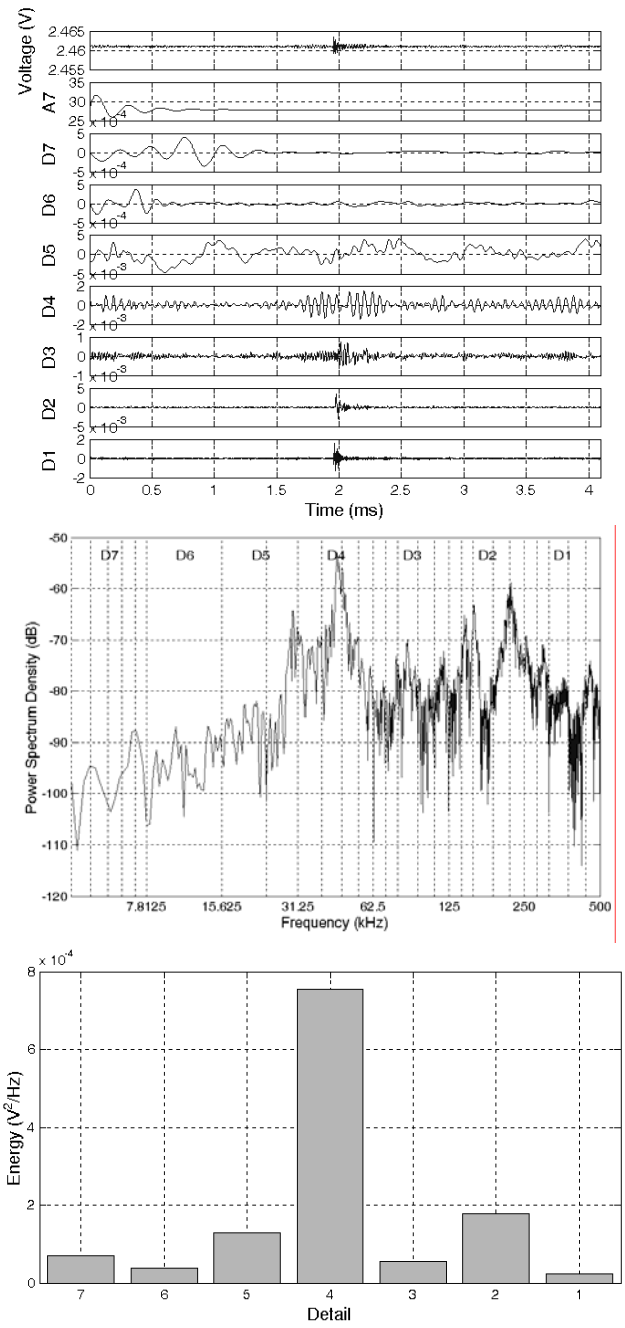

Fig. 14. DWT, PSD, the value of the energy transferred of a series of AE pulses generated by PDs in the surface system in air, during the positive voltage half-cycle.

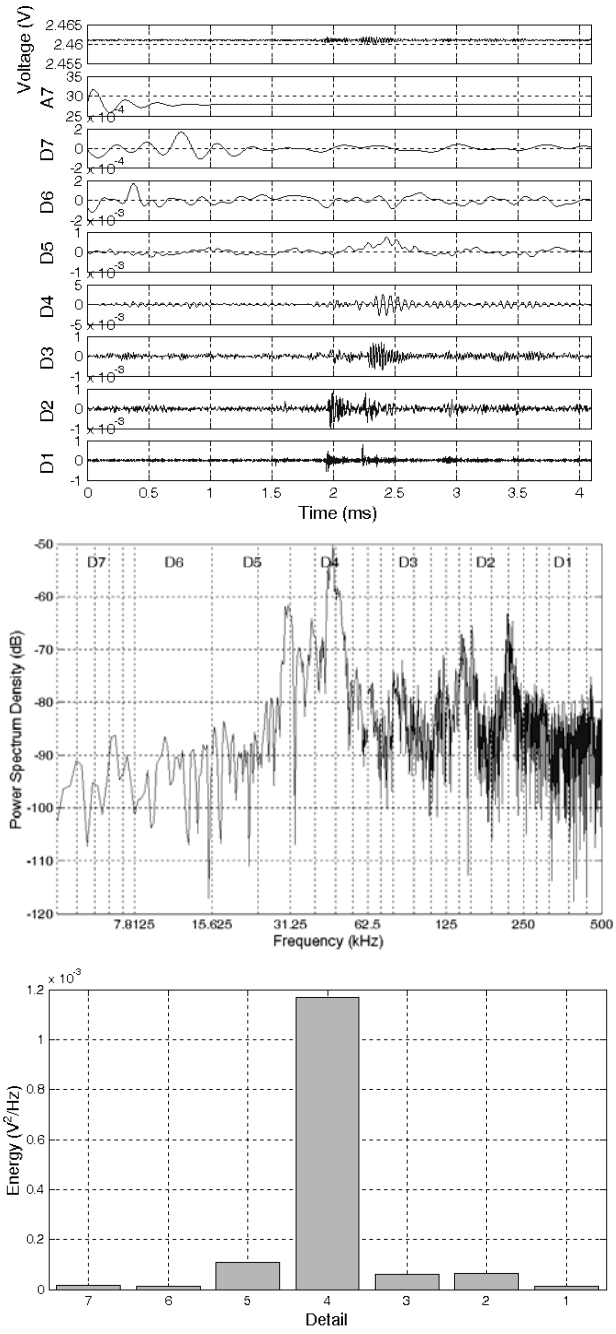

Fig. 15. Fig. DWT, PSD, the value of the energy transferred of a series of AE pulses generated by PDs in the surface system in air, during the negative voltage half-cycle.

broadened structures, the duration time of which is even longer than 0.6 ms. The biggest participation in the energy transferred by the AE pulses measured, for both voltage half-times, has Detail D4, but its value is by an order higher for the positive polarization.

The frequency characteristics do not contain resonance peaks, their median frequency is of 191.9 kHz, and the ranges of dominant frequencies, determined for the discrimination threshold equal to –70 dB, are within the ranges: (30-50) kHz, (140-160) kHz and (220-240) kHz for both voltage polarizations.

V. Summing-up

For the AE pulses generated by SPDs in air scalograms of a different character of the time-frequency structures determined for the positive and negative voltage polarizations were obtained. The calculation of wavelet distributions made it possible to obtain information on frequency structure changes in the particular stages of forming series of discharges. This

type of analysis is not possible when a frequency analysis using a Fourier transform is applied, for which the spectra obtained are averaged in the whole time range analyzed.

For the AE pulses generated by surface partial discharges (SPDs) in the positive and negative voltage half-times a similar shape to the power density spectrum runs was obtained. Moreover, an insignificant influence of the voltage polarization supplying the spark gap under study modeling SPDs on the results of the time-frequency analysis carried out using the STFT and DWT is obtained The results presented in this paper confirm the effectiveness of the time-frequency analysis as a calculation tool for identification of particular phases of PD forming in time that can occur on surfaces of both stationary and linear insulations. Therefore, the AE method can constitute an effective diagnostic method of non-destructive testing the degree of hazard to the surfaces of insulation materials by PDs.

[1] R. Aggarwal, C.H. Kim. Wavelet Transforms in Power Systems. Part 1. General Introduction to the Wavelet Transform // *Power Engineering Journal*, **April**, pp. 81-87 (2000).

[2] R. Aggarwal, C.H. Kim. Wavelet Transforms in Power Systems. Part 2. Examples of Application to Actual Power System Transients // *Power Engineering Journal*, **August**, pp. 193-202 (2001).

[3] R. Aggarwal, P.L. Mao. A Wavelet Transform Based Decision Making Logic Method for Discrimination Between Internal Faults and Inrush Currents in Power Transformers // *Electric Power and Energy Systems*, **22**, pp. 389-395 (2000).

[4] G. Andira, M. Savino, A. Trotta. Windows and Interpolation Algorithms to Improve Electrical Measurement Accuracy // *IEEE Trans. on Instrumentation and Measurement*, **38**, pp. 856-863 (1989).

[5] A. Antoniadis, G. Oppenheim. *Wavelets and Statistics.* Springer-Verlag, New York, (1995).

[6] L. Antoniou, K. Gustafson. Wavelets and Stochastic Processes // *Mathematics and Computers in Simulation,* **49**, pp. 81-104, (1999).

[7] F. Asamoah. Discrete Wavelet Analysis of Signals // *International Journal of Electrical Engineering Education*, **36**(3), pp. 255-265, (1999).

[8] T. Bengtsson, M. Leijon, L. Ming, B. Jonssn. Directivity of Acoustic Signals From PD in Oil // *IEE Proc. Sci. Meas. Technol.*, **142**(1), pp. 118-132 (1995).

[9] M. Beyer, H. Borsi, M. Hartje. Some Aspect About Possibilities and Limitation of Acoustic PD Measurements in Insulating Fluids. In book: *V Int. Symp. on High Vol. Eng. Braunschweig*, Germany, pp. 1-4 (1987).

[10] J.T. Białasiewicz. Falki i aproksymacje. WNT, Warszawa (2000).

[11] T. Boczar. Application of Signal Processing Elements for the Characteristics of AE Pulses Generated by PDs // *International Journal of Electrical Engineering Education (Great Britain),* in printing.

[12] T. Boczar. Application of the Correlation Methods for the Identification of Interfering Signals Accuring During the Measurements of PDs Using AE Method. *Proceedings 32nd International Conference, CNDT – Defektoskopie-2002*, Liberec, pp. 25-32 (2002).

[13] T. Boczar. Identification of fundamental forms of partial discharges based of the results of frequency analysis of their acoustic emission // *Journal of Acoustic Emission,* **17**(3-4), pp. S7-S12 (1999).

[14] T. Boczar. Identification of a Specific Type of Partial Discharges form Acoustic Emission Frequency Spectra // *IEEE Transactions on Dielectrics and Electrical Insulation*, **8**(4), pp. 598-606 (2001).

[15] R.N. Bracewell. *The Fourier Transform and its Applications*. McGRAW-HILL, International Editions (2000).

[16] L. Cohen. *Time-frequency Analysis*. Englewood Cliffs, Prentice Hall (1995).

[17] A. Cohen. *Wavelets and Multiscale Signal Processing*. Chapman&Hall, London (1995).

[18] I. Daubechies. *Ten Lectures on Wavelets*. Society for Industrial and Applied Mathematics, Philadelphia (1997).

[19] L. Debnath. *Wavelet Transforms and Time-Frequency Analysis*. Birkhauser, Boston (2001).

[20] R.A. Devore, B. Jawerth, B.J. Lucier. Image Compression Through Wavelet Transform Coding // *IEEE Trans. on Inf. Theory*, **38**(2), pp. 719-746 (1992).

[21] L.Z. Fang, R.L. Thews. *Wavelets in Physics*. Word Scientific, Singapore (1998).

[22] Z. Flisowski. *Technika wysokich napięć*. WNT, Warszawa (1995).

[23] B. Florkowska, M. Florkowski, R. Włodek, P. Zydroń. *Mechanizmy, pomiary i analiza wnz w diagnostyce układów izolacyjnych wysokiego napięcia.* IPPT PAN, Warszawa (2001).

[24] A.A. Girgis, E.B. Makram, T. Zheng. Power System Transient and Harmonic Studies Using Wavelet Transform // *IEEE Trans. on Power Delivery*, **14**(4), pp. 1461-1468 (1999).

[25] N. Hess-Nielsen, M.V. Wickerhauser. Wavelets and Time-Frequency Analysis // *Proceedings of the IEEE*, **84**(4), pp. 523-539 (1996).

[26] C.T. Hsiech, C.L. Huang, S.J. Huang. Application of Wavelets to Classify Power System Disturbances // *IEEE Trans. on Power Delivery*, **14**(47), pp. 87-93 (1998).

[27] G. Kaiser. *A Friendly Guide to Wavelets*. Birkhauser (1994).

[28] *Labview Measurements Manual.* National Instruments Corporate Headquarters, Austin, USA (2000).

[29] *Labview User Manual.* National Instruments Corporate Headquarters, Austin, USA (2000).
[30] C.H. Lee, A.P.S. Meliopoulos. An Alternative Method for Transient Analysis Via Wavelets // *IEEE Trans. on Power Delivery*, **15**(1), pp. 114-121 (2000).
[31] X. Ma, C. Zhou, I.J. Kemp. Interpretation of Wavelet Analysis and Its Application in PD Detection // *IEEE Trans. on Diel. and El. Ins.*, **9**(3), pp. 446-457 (2002).
[32] K. Masatake, T. Ampol. Detection of Wide-Band E-M Signals Emitted from PD Occuring in GIS Using Wavelet // *IEEE Trans. on Power Delivery*, **15**(2), pp. 467-472 (2002).
[33] Y. Nieverglet. *Wavelets Made Easy*. Birkhauser, Boston (1999).
[34] R.T. Ogden. *Essential Wavelets for Statistical Applications and Data Analysis*. Birkhauser (1997).
[35] V.L. Pham, K.P. Wong. Antidestruction Method for Wavelet Transform Filter Banks and Nonstationary Power System Waveform Harmonic Analysis // *IEE Processing Gener. Transm. Distrib.*, **148**(2), pp. 177-122 (2001).
[36] P. Purkait, S. Chakravorti. Pattern Classification of Impulse Faults in Transformers by Wavelet Analysis *IEEE Trans. on Diel. and El. Ins.*, **9**(4), pp. 555-562 (2002).
[37] O. Rioul, M. Vetterli. Wavelets and Signal Processing // *IEEE Signal Processing Magazine*, **October**, pp. 14-38 (1991).
[38] E. Rosołowski. *Cyfrowe przetwarzanie sygnałów w automatyce elektroenergetycznej*. Ak. Of. Wyd. EXIT, Warszawa (2002).
[39] Q. Shie, D. Chen. *Joint Time-Frequency Analysis: Methods and Applications*. Prentice Hall: Upper Saddle River (1996).
[40] G. Strang. Signal Processing for Everyone. *Computational Mathematics Driven by Industrial Problems*. Springer-Verlag, New York (2000).
[41] G. Strang, T. Nguyen. *Wavelets and Filter Banks*. Wellesley-Cambridge Press (1996).
[42] Z. Szczepański. *Wytrzymałość dielektryczna*. Skrypt Pol. Łódzka (1986).
[43] R. Tolimieri, A. Myoung. *Time-Frequency Representation*. Birkhauser, Boston (1998).
[44] L.K. Well. *The LabVIEW Student Edition Users's Guide*. Prentice Hall, Englewood Cliffs, New Jersey (1995).
[45] P. Wojtaszczyk. *Teoria falek*. Wyd. Naukowe PWN, Warszawa (2000).
[46] T.P. Zieliński. *Od teorii do cyfrowego przetwarzania sygnałów*. Wydz. EAIiE AGH Kraków (2002).
[47] P. Zydroń. *Wybrane zagadnienia analizy czasowo częstotliwościowej wyładowań niezupełnych*. WEAIiE AGH, Kraków (2001).
[48] R. Zydroń, P. Włodek. Application of signal processing elements to partial discharges detection, mesurements and analysis. *Conference Processing 10th ISH*. Montreal, Canada, Cd file 3437, (1997).
[49] P. Zydroń, R. Włodek. Elements of signal theory in detection of partial discharges for diagnostics aims. *8th Workshop on High Voltage Engineering*. The Institute of power Transmission and High Voltage Technique, University of Stuttgart, Hirschegg (1996).

Т. Боцар

Результати частотно-часового аналізу емісії акустичних імпульсів, створюваних зовнішніми частковими розрядами у повітрі

Технічний університет Ополе, Польща

Предметом статті є проблеми, спільні з використанням сучасних цифрових методів обробки і аналізу сигналів, виміряних методом акустичної емісії (AE) протягом проведення високоенергетичних експериментів в лабораторних умовах при змодельованих зовнішніх часткових розрядах (PDs) у повітрі.

Насамперед у статті представлено результати частотно-часового аналізу імпульсів AE, які генеруються PDs використовуючи неперервні (CWT) і дискретні (DWT) хвилі.